*Journal of Sound and Vibration* (1999) **228**(3), 611–628
*Article No.* jsvi.1999.2423, available online at http://www.idealibrary.com on IDEAL®

# VIBRATION OF MULTI-SPAN NON-UNIFORM BRIDGES UNDER MOVING VEHICLES AND TRAINS BY USING MODIFIED BEAM VIBRATION FUNCTIONS

Y. K. CHEUNG, F. T. K. AU, D. Y. ZHENG AND Y. S. CHENG

*Department of Civil Engineering, The University of Hong Kong, Pokfulam Road, Hong Kong, Peoples Republic of China*

(*Received* 30 *August* 1997, *and in final form* 7 *June* 1999)

Based on the Lagrangian approach, the vibration of a multi-span non-uniform bridge subjected to a moving vehicle is analyzed by using modified beam vibration functions as the assumed modes. The vehicle is modelled as a two-degree-of-freedom system. The method is extended to the action of a moving train by modelling it as a series of two-degree-of-freedom systems. All the derived formulae are expressed in matrix form and therefore programming is quite straightforward. The total number of unknowns for this method is very small compared with that of the finite element method. Convergence is very quick and in almost all cases 12–16 terms are sufficient to give satisfactory results.



## 1. INTRODUCTION

The dynamic response of bridge structures subjected to moving vehicles and trains has long been an interesting topic in the field of civil engineering. In early studies, a moving-force model was used where the inertia of the vehicle was small compared to that of the bridge, whereas a moving-mass model was used instead where the inertia of the vehicle could not be taken as small. With the large increase in the proportion of heavy vehicles and high-speed vehicles in highway and railway traffic, the interaction problem between vehicles and bridge structures has attracted much attention during the last two decades. Two kinds of methods, i.e., analytical and numerical methods, are widely used to tackle the problem. Fryba [1] presented in his monograph various analytical solutions for vibration problems of simple structures under moving vehicles. As analytical methods are often limited to simple moving load problems, many researchers have resorted to various numerical methods [2–12].

The finite element method is one of the most versatile numerical methods used by many researchers. Yoshida and Weaver [2] first applied it to the moving load problem. Filho [3] also used it to analyze the dynamic response of a simply supported beam subjected to a constant-velocity two-degree-of-freedom (2-d.o.f.) vehicle with various mass ratios. Later, Hino *et al.* [4] analyzed the dynamic response of a concrete bridge of non-uniform sections subjected to a moving load.

0022-460X/99/480611 + 18 $30.00/0 

The bridge was modelled as a double cantilever beam with a small suspended span, and the moving vehicle was assumed to be a single d.o.f. spring–mass–damper system. The Galerkin method, a form of method of the weighted residuals, was used for the formulation and the Wilson $\theta$ method [13] was adopted to solve the dynamic equations. Hino *et al.* [5] further extended the method to the solution of geometric non-linear vibration of beams with simply supported and clamped ends, in which the moving vehicle was modelled as a 2-d.o.f. one-foot dynamic system. The non-linear equations derived were then linearized by means of the incremental method and the transitional response was calculated by the Newmark $\beta$ method [13].

Subsequently, Olsson [6] derived a general bridge-vehicle element to solve the dynamic interaction problem. The bridge response was formulated in modal co-ordinates thereby reducing the number of equations to be solved within each time step. He computed, as illustrative examples, the dynamic magnification factors of a simply supported beam with or without surface irregularities subjected to a moving one-axle vehicle. Later, Lin and Trethewey [7] computed the dynamic response of elastic beams subjected to a moving dynamic load with a constant velocity or with a general movement profile by using the finite element method and the Runge–Kutta technique. The moving dynamic load was modelled as either a one-foot or a two-foot dynamic system.

Yener and Chompooming [8] used the method of lines [14] to study the vehicle–bridge dynamic interaction problem. In their study, the governing partial differential equations of the vehicle–bridge system were first changed into a set of ordinary differential equations by spatial discretization based on the finite element method. Then step-by-step integration in time domain was applied to solve these matrix ordinary differential equations. The moving vehicle was modelled as either a one-dimensional moving mass model with 3 d.o.f.s or a two-dimensional moving mass model with 6 d.o.f.s. They later extended the method to investigate the effects of roadway surface irregularities and vehicle deceleration on bridge dynamics [9].

In a separate development, Yang and Lin [10] presented a vehicle–bridge interaction element in which the deck element and the parts of the car body in contact were regarded as a substructure. All the d.o.f.s associated with the car body within each substructure were first eliminated by means of the dynamic condensation method [15] and then the Newmark $\beta$ method was used to solve the equations of motion. Then they further applied the method to analyze the impact effects of simply supported beams and three-span continuous beams subjected to a moving five-axle truck modelled as three lumped masses resting on three sets of springs and dashpots [11].

However, the number of unknowns involved and the amount of input data are very large in the finite element method. This paper presents a method in which the number of unknowns is substantially reduced. In this method, the modified beam vibration functions are chosen as the assumed modes of a multi-span bridge and the Lagrangian approach is used to solve the interaction problem. The modified beam vibration functions, which have been used to solve the moving force problem [16], satisfy the zero deflection conditions at all the intermediate point supports as well as the boundary conditions at the two ends of the bridge. The whole multi-span

bridge can be considered as one single "element" in the formulation. This method converges very quickly and, in almost all cases, 12–16 terms are sufficient to obtain accurate results.

## 2. THEORY AND FORMULATION

A continuous linear elastic Bernoulli–Euler bridge with $(Q + 1)$ point supports subjected to a convoy comprising $N$ moving vehicles is shown in Figure 1. The vehicles are modelled as moving systems each of 2 d.o.f.s $\{M_{s1}, M_{s2}, c_s, k_s, s = 1, 2, \ldots, N\}$ and they move as a group at a prescribed velocity $v(t)$ along the axial direction from left to right. Here $M_{s1}$ and $M_{s2}$ are the unsprung mass and sprung mass of the $s$th vehicle respectively. The two masses are interconnected by a spring of stiffness $k_s$ and a dashpot of damping coefficient $c_s$. The horizontal position of the $s$th vehicle measured from the left end of the bridge is $x_s(t)$, a function of time $t$. A moving train can therefore be treated as a special case with a series of 2-d.o.f. systems arranged in a regular pattern to represent the wheel assemblies. The deflection of the bridge is denoted by $w(x, t)$ where upward deflection is taken as positive. The vertical displacement of the masses $M_{s1}$ and $M_{s2}$ and $y_{s1}(t)$ and $y_{s2}(t)$, respectively, and they are measured vertically upward with reference to their respective vertical equilibrium positions before coming onto the bridge. If the surface roughness of the bridge $r(x)$ is defined as the vertically upward departure from the mean horizontal profile, then the vertical displacement $y_{s1}(t)$ of the unsprung mass of the $s$th vehicle and its first and second derivatives are as follows:

$$y_{s1}(t) = [w(x, t) + r(x)]|_{x = x_s(t)}, \tag{1}$$

$$\frac{\mathrm{d}y_{s1}(t)}{\mathrm{d}t} = \left[\frac{\partial w}{\partial t} + v\frac{\partial w}{\partial x} + v\frac{\mathrm{d}r}{\mathrm{d}x}\right]\Bigg|_{x = x_s(t)}, \tag{2}$$

$$\frac{\mathrm{d}^2 y_{s1}(t)}{\mathrm{d}t^2} = \left[\frac{\partial^2 w}{\partial t^2} + 2v\frac{\partial^2 w}{\partial x \partial t} + v^2\frac{\partial^2 w}{\partial x^2} + a\frac{\partial w}{\partial x} + v^2\frac{\mathrm{d}^2 r}{\mathrm{d}x^2} + a\frac{\mathrm{d}r}{\mathrm{d}x}\right]\Bigg|_{x = x_s(t)}, \tag{3}$$

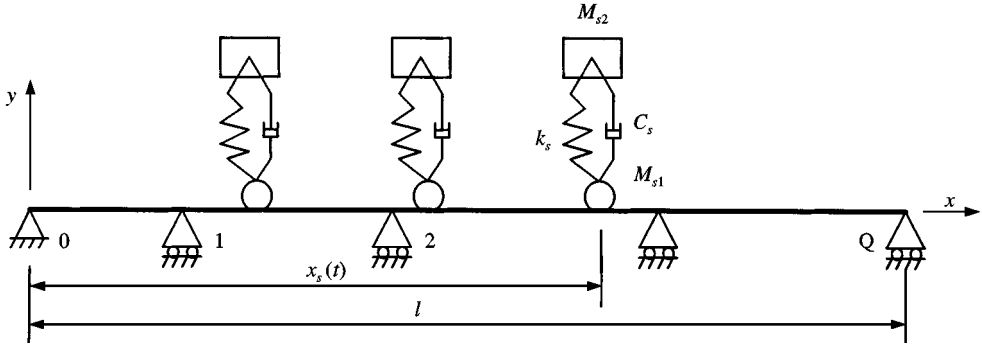


Figure 1. A continuous beam with $(Q - 1)$ intermediate point supports under $N$ moving vehicles.

where $a$ is the horizontal acceleration of the convoy of vehicles. Notice that the independent variables are omitted for simplicity. The contact force between the $s$th vehicle and the bridge is denoted by $f_{cs}(t)$, and it can be expressed as

$$f_{cs}(t) = (M_{s1} + M_{s2})g + \Delta f_{cs}(t), \tag{4}$$

in which $g$ is the acceleration due to gravity and $\Delta f_{cs}(t)$ is the time-dependent variation of contact force.

The equations of vertical motion for the masses $M_{s1}$ and $M_{s2}$ can be written as

$$M_{s1}\frac{\mathrm{d}^2 y_{s1}(t)}{\mathrm{d}t^2} = \Delta f_{cs}(t) + k_s[y_{s2}(t) - y_{s1}(t)] + c_s\left[\frac{\mathrm{d}y_{s2}(t)}{\mathrm{d}t} - \frac{\mathrm{d}y_{s1}(t)}{\mathrm{d}t}\right], \tag{5}$$

$$M_{s2}\frac{\mathrm{d}^2 y_{s2}(t)}{\mathrm{d}t^2} = -k_s[y_{s2}(t) - y_{s1}(t)] - c_s\left[\frac{\mathrm{d}y_{s2}(t)}{\mathrm{d}t} - \frac{\mathrm{d}y_{s1}(t)}{\mathrm{d}t}\right]. \tag{6}$$

From equations (4)–(6), the contact force $f_{cs}(t)$ becomes

$$f_{cs}(t) = (M_{s1} + M_{s2})g + M_{s1}\frac{\mathrm{d}^2 y_{s1}(t)}{\mathrm{d}t^2} + M_{s2}\frac{\mathrm{d}^2 y_{s2}(t)}{\mathrm{d}t^2}. \tag{7}$$

The vibration of the bridge $w(x, t)$ can be expressed as

$$w(x, t) = \sum_{i=1}^{n} q_i(t) X_i(x), \tag{8}$$

where $\{q_i(t), i = 1, 2, \ldots, n\}$ are generalized co-ordinates and $\{X_i(x), i = 1, 2, \ldots, n\}$ are the assumed vibration modes which satisfy the boundary conditions *a priori* (see reference [16]). The assumed vibration modes can be written as

$$X_i(x) = \bar{X}_i(x) + \tilde{X}_i(x), \tag{9}$$

where $\{\bar{X}_i(x), i = 1, 2, \ldots, n\}$ are the vibration modes of a hypothetical prismatic beam of total length $l$ with the same end supports but without the intermediate supports, and $\{\tilde{X}_i(x), i = 1, 2, \ldots, n\}$ are the augmenting cubic spline expressions which are so chosen that each $X_i(x)$ satisfies the boundary conditions at the two ends and the zero deflection conditions at the intermediate point supports. The vibration modes $\bar{X}_i(x)$ are Fourier sine series for a simply supported beam, and those for other end conditions are given in reference [17]. Notice that cubic spline expressions are chosen instead of a higher order polynomial so that convergence is faster.

The Lagrangian equation of the bridge is written in terms of the Lagrangian function $L$ and the generalized force $Q_{is}^*(t)$ as

$$\frac{\mathrm{d}}{\mathrm{d}t}\left(\frac{\partial L}{\partial \dot{q}_i}\right) - \frac{\partial L}{\partial q_i} = \sum_{s=1}^{N} Q_{is}^*(t), \quad i = 1, 2, \ldots, n. \tag{10}$$

The Lagrangian function $L$ can be written as

$$L = V - U, \tag{11}$$

in terms of the kinetic energy $V$ and the bending energy $U$ which are explicitly given by

$$V = \frac{1}{2}\int_0^l \rho A(x)\left[\frac{\partial w(x,t)}{\partial t}\right]^2 \mathrm{d}x, \tag{12}$$

$$U = \frac{1}{2}\int_0^l EI(x)\left[\frac{\partial^2 w(x,t)}{\partial x^2}\right]^2 \mathrm{d}x, \tag{13}$$

where $\rho$ is the density, $E$ is the Young's modulus, $A(x)$ is the area, $I(x)$ is the moment of inertia of the cross-section. Substituting equation (8) into equations (12) and (13), we get, respectively,

$$V = \frac{1}{2}\sum_{i=1}^{n}\sum_{j=1}^{n}\dot{q}_i(t)m_{ij}\dot{q}_j(t), \tag{14}$$

$$U = \frac{1}{2}\sum_{i=1}^{n}\sum_{j=1}^{n}q_i(t)k_{ij}q_j(t), \tag{15}$$

in which

$$m_{ij} = \int_0^l \rho A(x)X_i(x)X_j(x)\,\mathrm{d}x, \tag{16}$$

$$k_{ij} = \int_0^l EI(x)X_i''(x)X_j''(x)\,\mathrm{d}x, \tag{17}$$

are the generalized mass and stiffness matrices of the bridge, respectively, the dot stands for differentiation with respect to time and the dash denotes differentiation with respect to $x$. The corresponding generalized force $Q_{is}^*(t)$ for the contact force $f_{cs}(t)$ can be expressed as

$$Q_{is}^*(t) = -f_{cs}(t)X_i(x)|_{x=x_s(t)}. \tag{18}$$

An explicit expression for the generalized force $Q_{is}^*(t)$ can be obtained from equations (7) and (18) as

$$\begin{aligned} Q_{is}^*(t) = &-(M_{s1}+M_{s2})gX_i(x_s(t)) - M_{s1}X_i(x_s(t))(v^2r''(x_s(t)) + ar'(x_s(t))) \\ &- M_{s1}X_i(x_s(t))\sum_{j=1}^{n}\{\ddot{q}_j(t)X_j(x_s(t)) + 2v\dot{q}_j(t)X_j'(x_s(t)) + q_j(t)[v^2X_j''(x_s(t)) \\ &+ aX_j'(x_s(t))]\} - M_{s2}\ddot{y}_{s2}(t)X_i(x_s(t)). \end{aligned} \tag{19}$$

The equation of motion for the bridge are obtained by substituting equations (11), (14), (15) and (19) into equation (10) as

$$\sum_{j=1}^{n} m_{ij}^{*}\ddot{q}_j(t) + \sum_{j=1}^{n} c_{ij}^{*}\dot{q}_j(t) + \sum_{j=1}^{n} k_{ij}^{*}q_j(t) + \sum_{s=1}^{N} M_{s2}X_i(x_s(t))\ddot{y}_{s2}(t) = p_i^{*}(t), \quad i = 1, 2, \ldots, n, \tag{20}$$

where

$$m_{ij}^{*}(t) = m_{ij} + \sum_{s=1}^{N} M_{s1}X_i(x_s(t))X_j(x_s(t)), \tag{21}$$

$$c_{ij}^{*}(t) = \sum_{s=1}^{N} 2vM_{s1}X_i(x_s(t))X_j'(x_s(t)), \tag{22}$$

$$k_{ij}^{*}(t) = k_{ij} + \sum_{s=1}^{N} M_{s1}X_i(x_s(t))[v^2X_j''(x_s(t)) + aX_j'(x_s(t))], \tag{23}$$

$$p_i^{*}(t) = -\sum_{s=1}^{N} [(M_{s1} + M_{s2})gX_i(x_s(t)) + M_{s1}X_i(x_s(t))(v^2r''(x_s(t)) + ar'(x_s(t)))]. \tag{24}$$

Note that in the derivation of the above equations, it has been assumed that all $N$ vehicles are acting on the bridge. Should a particular vehicle be outside the bridge, the corresponding terms under the summation signs should be omitted.

From equation (6), the equation of motion of the sprung mass $M_{s2}$, we have

$$-\sum_{j=1}^{n} c_sX_j(x_s(t))\dot{q}_j(t) - \sum_{j=1}^{n} [k_sX_j(x_s(t)) + vc_sX_j'(x_s(t))]q_j(t) + M_{s2}\ddot{y}_{s2}(t) + c_s\dot{y}_{s2}(t) + k_sy_{s2}(t) = k_sr(x_s(t)) + vc_sr'(x_s(t)), \quad s = 1, 2, \ldots, N. \tag{25}$$

The above equation is only valid when the $s$th vehicle acts on the bridge.

Equations (20) and (25) can be written together in matrix form as

$$\begin{bmatrix} \mathbf{M}^{*} & \mathbf{X}\mathbf{M}_2 \\ 0 & \mathbf{M}_2 \end{bmatrix} \begin{Bmatrix} \ddot{\mathbf{q}} \\ \ddot{\mathbf{y}}_2 \end{Bmatrix} + \begin{bmatrix} \mathbf{C}^{*} & \mathbf{0} \\ -\mathbf{C}\mathbf{X}^{\mathrm{T}} & \mathbf{C} \end{bmatrix} \begin{Bmatrix} \dot{\mathbf{q}} \\ \dot{\mathbf{y}}_2 \end{Bmatrix} + \begin{bmatrix} \mathbf{K}^{*} & \mathbf{0} \\ -\mathbf{K}\mathbf{X}^{\mathrm{T}} - v\mathbf{C}\mathbf{X}'^{\mathrm{T}} & \mathbf{K} \end{bmatrix} \begin{Bmatrix} \mathbf{q} \\ \mathbf{y}_2 \end{Bmatrix} = \begin{Bmatrix} \mathbf{p}^{*} \\ \mathbf{K}\mathbf{r} + v\mathbf{C}\mathbf{r}' \end{Bmatrix}, \tag{26}$$

where the sub-matrices are given below in terms of the typical element at the $i$th row and the $j$th column, and the sub-vectors are given in terms of the typical $i$th element

$$\mathbf{M}^{*} = [m_{ij}^{*}(t)], \quad i, j = 1, 2, \ldots, n, \tag{27}$$

$$\mathbf{C}^* = [c_{ij}^*(t)], \quad i, j = 1, 2, \ldots, n, \tag{28}$$

$$\mathbf{K}^* = [k_{ij}^*(t)], \quad i, j = 1, 2, \ldots, n, \tag{29}$$

$$\mathbf{p}^* = \{p_i^*(t)], \quad i = 1, 2, \ldots, n, \tag{30}$$

$$\mathbf{M}_2 = diag[M_{i2}], \quad i = 1, 2, \ldots, N, \tag{31}$$

$$\mathbf{C} = diag[c_i], \quad i = 1, 2, \ldots, N, \tag{32}$$

$$\mathbf{K} = diag[k_i], \quad i = 1, 2, \ldots, N, \tag{33}$$

$$\mathbf{X} = [X_i(x_j(t))], \quad i = 1, 2, \ldots, n, \quad j = 1, 2, \ldots, N, \tag{34}$$

$$\mathbf{r} = \{r(x_i(t))\}, \quad i = 1, 2, \ldots, N, \tag{35}$$

$$\mathbf{q} = \{q_i(t)\}, \quad i = 1, 2, \ldots, n, \tag{36}$$

$$\mathbf{y}_2 = \{y_{i2}(t)\}, \quad i = 1, 2, \ldots, N. \tag{37}$$

Equation (26) can then be solved by the Wilson-$\theta$ method [13]. However, this equation has been written on the assumption that all $N$ vehicles are acting on the bridge. Where a certain vehicle is not on the bridge, the corresponding rows and columns of the matrix equation should be deleted.

## 3. RESULTS AND SIMULATIONS

The method of solution is demonstrated by application to the following examples. The present results are compared with either published results where applicable or results obtained using the finite element method [18].

### 3.1. EXAMPLE 1. A SINGLE-SPAN SIMPLY SUPPORTED BRIDGE UNDER A MOVING VEHICLE [6]

The single-span simply supported bridge as shown in Figure 2 is assumed to have a harmonically varying surface irregularity represented by

$$r(x) = (d/2)[1 - \cos(2\pi x/\bar{l})],$$

where $d$ and $\bar{l}$ are the surface irregularity depth and length respectively. A vehicle, which is modelled as an unsprung mass $m_1$ and a sprung mass $m_2$ connected by a spring with stiffness $k$ and a damper with damping coefficient $c$, is assumed to move with a constant speed $v$ along the bridge. In parallel with the notations used

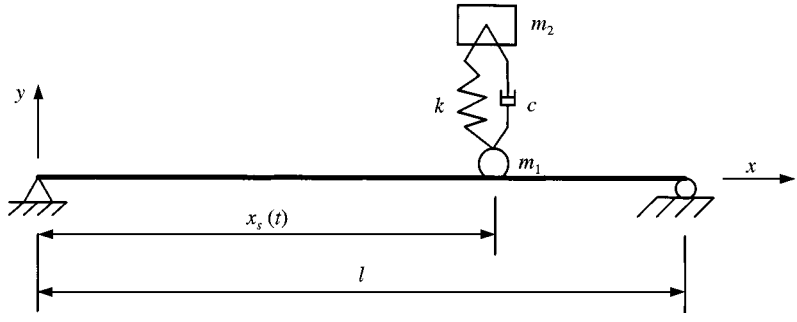


Figure 2. A single-span simply supported bridge under a single-axle moving vehicle.

in reference [6], seven dimensionless parameters are defined as follows:

velocity ratio, $\alpha = v\pi/\omega_{b,1} l$, where $\omega_{b,1} = \pi^2\sqrt{EI/\rho A l^4}$;
unsprung to sprung mass ratio, $\kappa_0 = m_1/m_2$;
vehicle to bridge mass ratio, $\kappa = (m_1 + m_2)/\rho A l$;
bridge to vehicle frequency ratio, $\Omega = \omega_{b,1}/\omega_v$, where $\omega_v = \sqrt{k/m_2}$;
vehicle damping ratio, $\xi_v = c/2m_2\omega_v$;
surface irregularity depth ratio, $r_d = 48EId/(m_1 + m_2)gl^3$; and
surface irregularity length ratio, $r_i = l/\bar{l}$.

The velocity ratio $\alpha$ is defined in such a way that, when $\alpha$ equals unity, the vehicle traversing time $\tau = l/v$ equals half the fundamental period of the bridge.

For comparison with reference [6], the following specific parameters are assumed; $\kappa = 0{\cdot}5$, $\kappa_0 = 0{\cdot}25$, $\Omega = 3$ and $\xi_v = 0{\cdot}125$. Various cases of the velocity ratios $\alpha$ and roughness are considered. The problem was solved by the present method using eight terms and 200 equal time steps. The same problem was also solved by finite element method using 16 beam elements and 200 equal time steps [18] for further comparison. In the presentation of results, the dynamic magnification factors for mid-span displacement $D_d$ and mid-span bending moment $D_m$ are defined as

$D_d$ = (maximum dynamic mid-span displacement)/(static mid-span displacement); and

$D_m$ = (maximum dynamic mid-span moment)/(static mid-span moment),

where the static quantities equal $-(m_1 + m_2)gl^3/48EI$ and $(m_1 + m_2)gl/4$, respectively, due to a concentrated load $(m_1 + m_2)g$ placed at mid-span.

A perfectly smooth bridge (i.e., $r_d = r_l = 0$) was first analyzed, and Figures 3 and 4 show the dynamic magnification factors $D_d$ and $D_m$, respectively, for the range of velocity ratio $0 \leqslant \alpha \leqslant 1{\cdot}0$. Figure 5 shows the contact force ratio $f_c(t)/(m_1 + m_2)g$ for the particular case $\alpha = 0{\cdot}25$. Then the same bridge with roughness ($r_d = 0{\cdot}05$, $r_l = 10$) was studied, and the dynamic magnification factors $D_d$ and $D_m$ for the range of velocity ratio $0 \leqslant \alpha \leqslant 0{\cdot}5$ are shown in Figures 6 and 7 respectively. In general, good agreement is observed among the present results, the finite element

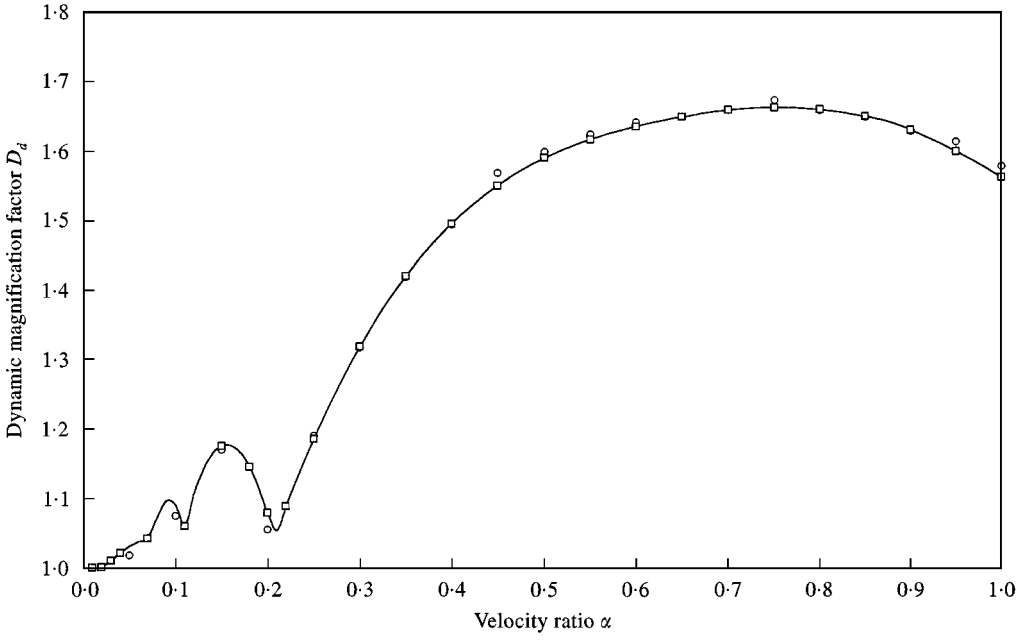


Figure 3. Simply supported bridge without roughness, dynamic magnification factor $D_d$. ——, present; ○, reference [6]; □, finite element [18].

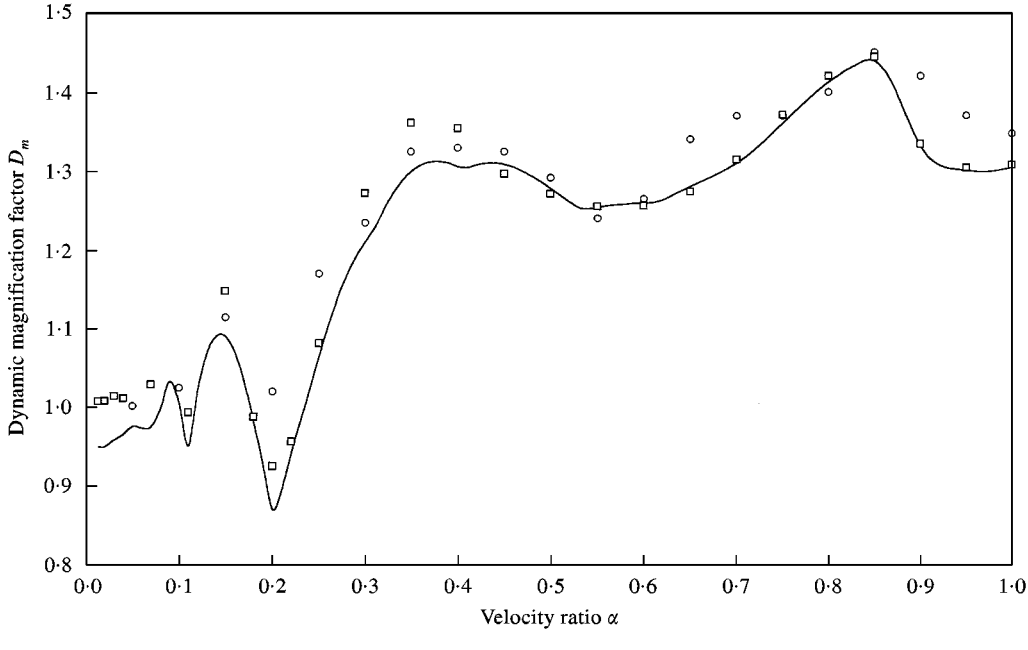


Figure 4. Simply supported bridge without roughness, dynamic magnification factor $D_m$. ——, present; ○, reference [6]; □, finite element [18].

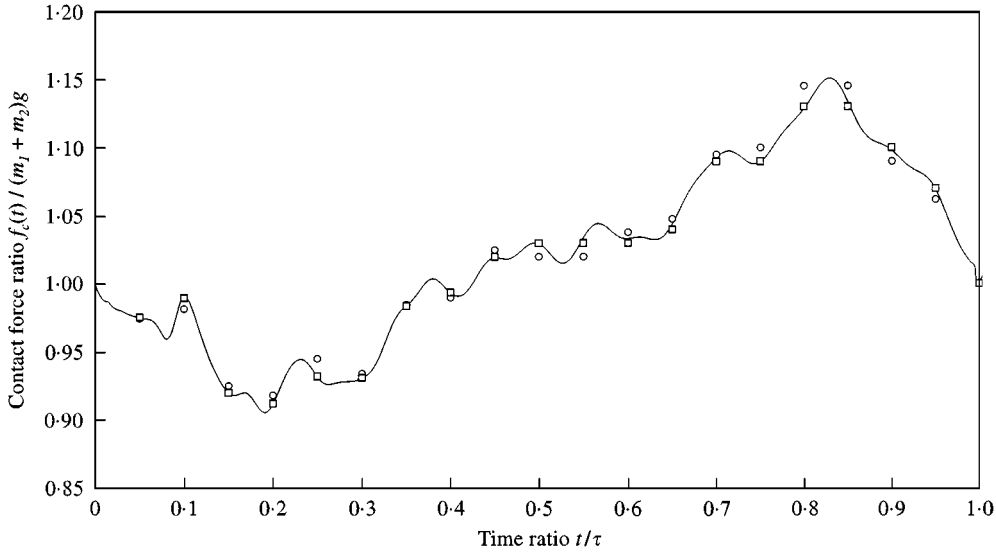


Figure 5. Simply supported bridge without roughness, contact force ratio for $\alpha = 0{\cdot}25$: ——, present; ○, reference [6]; □, finite element [18].

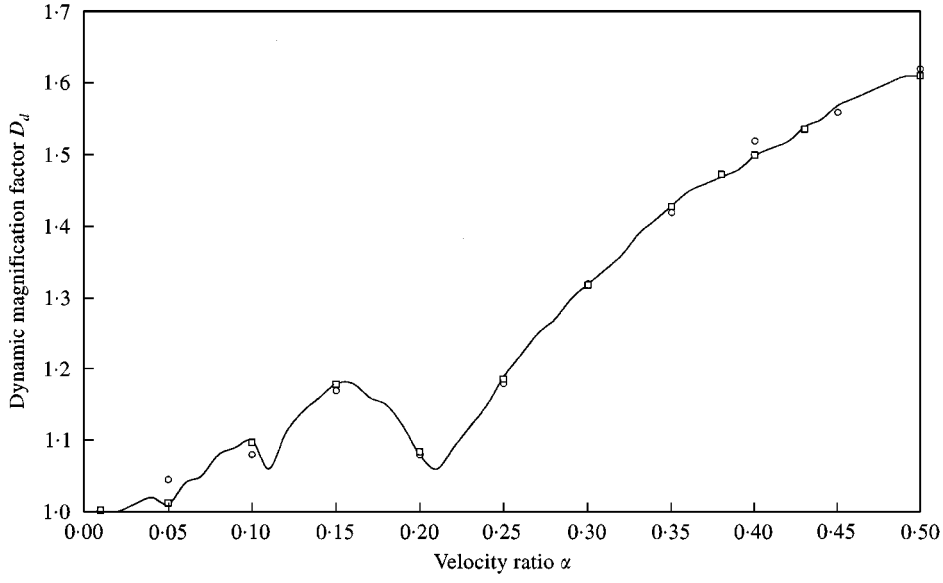


Figure 6. Simply supported bridge with roughness d($r_d = 0{\cdot}05, r_l = 10$), dynamic magnification factor $D_d$: ——, present; ○, reference [6]; □, finite element [18].

results [18] and those due to Olsson [6]. However, some discrepancies in the results for the dynamic magnification factor $D_m$ are noticed as the computed bending moment, being proportional to the second derivative of the deflection with respect to co-ordinate $x$, is dependent on the numerical method used.

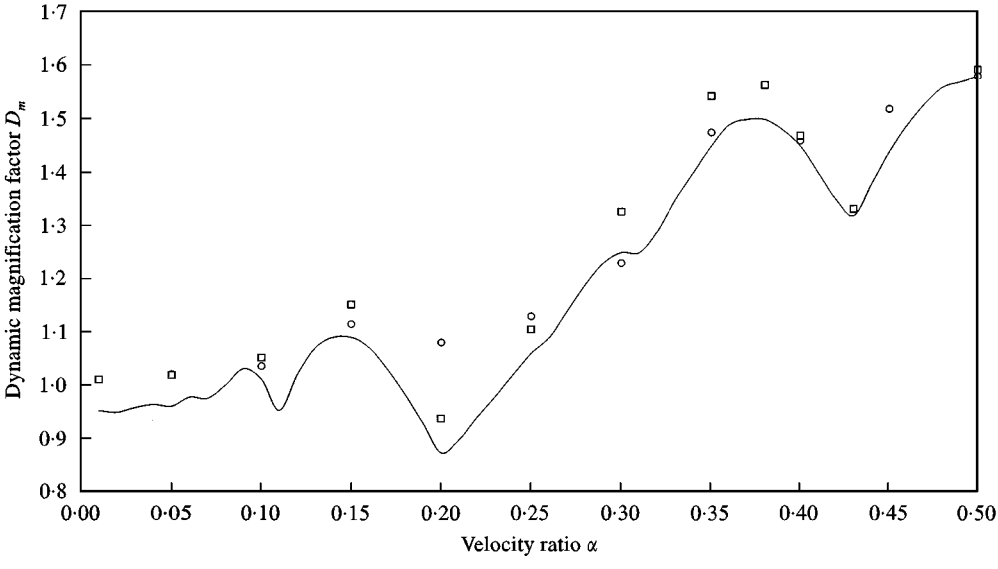


Figure 7. Simply supported bridge with roughness ($r_d = 0{\cdot}05, r_l = 10$), dynamic magnification factor $D_m$: ——, present; ○, reference [6]; □, finite element [18].

### 3.2. EXAMPLE 2. A THREE-SPAN CONTINUOUS BOX GIRDER BRIDGE OF PARABOLIC SOFFIT UNDER A MOVING VEHICLE

Figure 8 shows a three-span continuous box girder bridge under a moving vehicle. The density $\rho$ and Young's modulus $E$ of concrete are 2400 kg/m$^3$ and 30 000 MPa respectively. The vehicle was modelled as a single-axle system with unsprung mass $m_1$ of 4800 kg, sprung mass $m_2$ of 27 000 kg, spring stiffness $k$ of $9{\cdot}12 \times 10^6$ N/m and damping coefficient $c$ of $8{\cdot}6 \times 10^4$ Ns/m, and the vehicle travels at a horizontal speed $v$ of 17 m/s across the bridge. The problem was solved by the present method using 12 terms and 240 equal time steps. The history curve for deflection $w$ at the middle of the central span of the bridge is plotted against $t/\tau$ in Figure 9, where $\tau$ is the vehicle traversing time. It is also compared with results from finite element method [18] using 120 beam elements and 240 equal time steps. Very good agreement is observed.

The same bridge was then analyzed assuming that a convoy comprising four of the above single-axle vehicles at regular spacing of 10 m moves at a constant speed $v$ of 17 m/s across the bridge. In this case, the vehicle traversing time $\tau$ is counted from the instant when the front vehicle arrives at the bridge to the instant when the last vehicle leaves it. The corresponding history curve for deflection is shown in Figure 10. Very good agreement is again observed.

### 3.3. A SINGLE-SPAN SIMPLY SUPPORTED BRIDGE UNDER A MOVING TRAIN [12]

Consider a single-span supported prestressed concrete bridge with a span of 20 m, second moment of area of cross-section I of 3·81 m$^4$, Young's modulus $E$ of

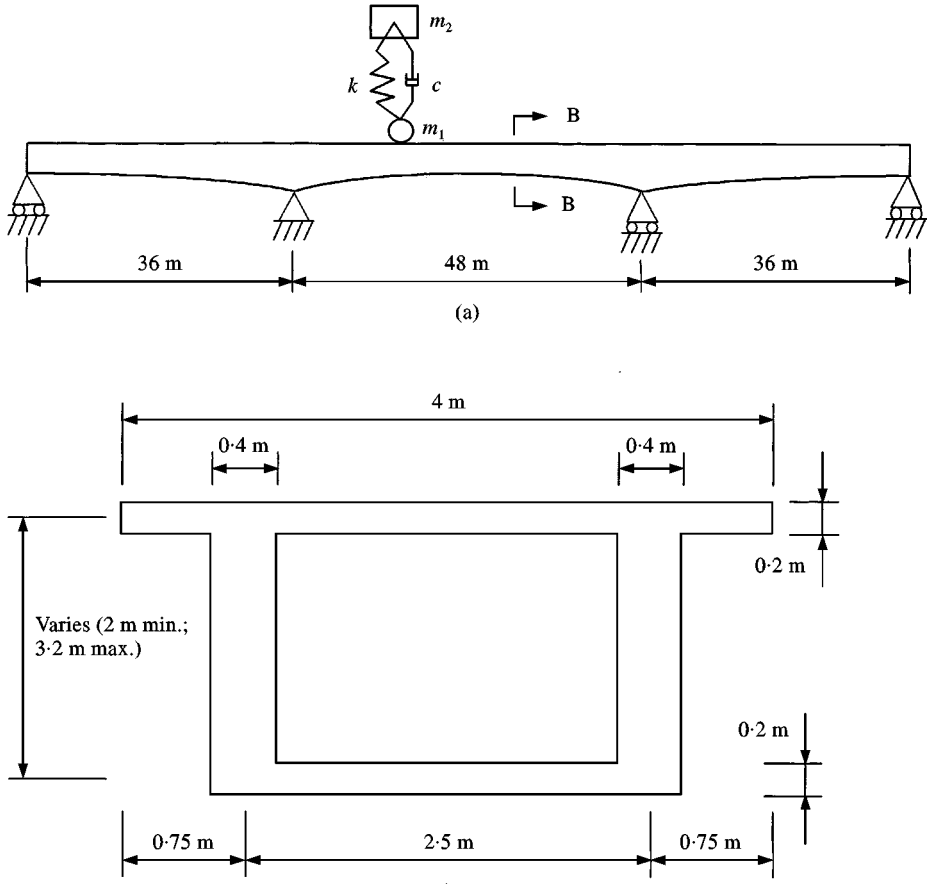


Figure 8. A three-span continuous bridge of parabolic soffit under a moving vehicle. (a) Elevation; (b) Section BB.

concrete of 29 430 MPa and a mass per unit length of 34 088 kg/m, for which the fundamental frequency is $\omega_I = 44{\cdot}75$ rad/s. A train consisting of 5 cars, as shown in Figure 11, runs over the bridge. In the moving force model, the loads from the front and rear wheel assemblies of each car are represented by two two moving forces, as shown in Figure 11(b). To account for the inertial effects as well, each car can be considered as comprising two 2-d.o.f. vehicles, as shown in Figure 11(c). Each wheel assembly is modelled as an equivalent 2-d.o.f. system with unsprung mass $m_1$ of 4400 kg, sprung mass $m_2$ of 17 600 kg, spring stiffness $k$ of $9{\cdot}12 \times 10^6$ N/m and damping coefficient $c$ of $8{\cdot}6 \times 10^4$ N s/m. The weight of each wheel assembly is therefore $P = 215{\cdot}6$ kN. The arrangement of wheel assemblies is defined by the parameters $L_c = 18$ m and $L_d = 6$ m. The velocity ratio $\alpha$ is taken as $\alpha = v\pi/\omega_I L$.

The train was first modelled as a series of moving forces and solved by the present method omitting the inertial terms of the vehicles using 12 terms and 2000 equal time steps. Figure 12 compares the dynamic magnification factor for mid-span displacement $D_d$ obtained from the present method with those by Yang *et al.* [12], indicating very good agreement. Effectively the same resonant points have

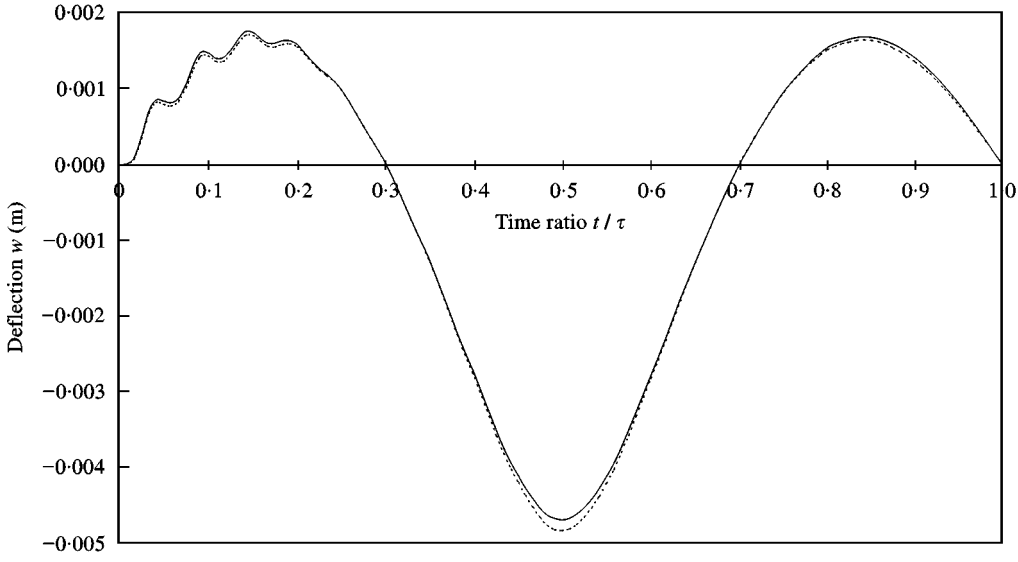


Figure 9. Three span continuous bridge under a single vehicle, deflection at middle of central span: ——, present; - - - - -, finite element [18].

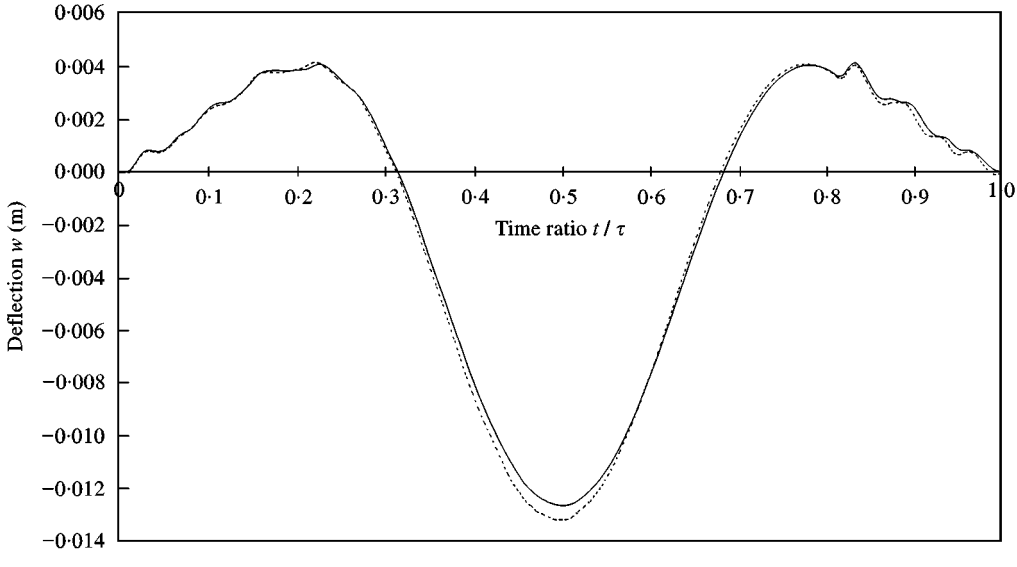


Figure 10. Three span continuous bridge under a convoy, deflection at middle of central span: ——, present; - - - - -, finite element [18].

been obtained. The problem was subsequently reanalyzed using the present method by the moving vehicle model also with 12 terms and 2000 equal time steps. The dynamic magnification factor $D_d$ is shown in Figure 13 and compared to result obtained from the finite element method [18] using 16 beam elements of equal lengths. Very good agreement is observed. Both the moving force model and the

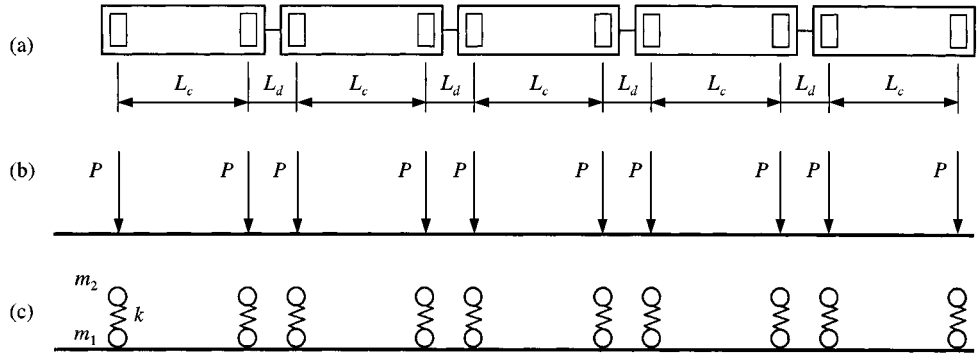


Figure 11. A moving train and its mathematical models (a) Plan; (b) Moving force model; (c) Moving vehicle model.

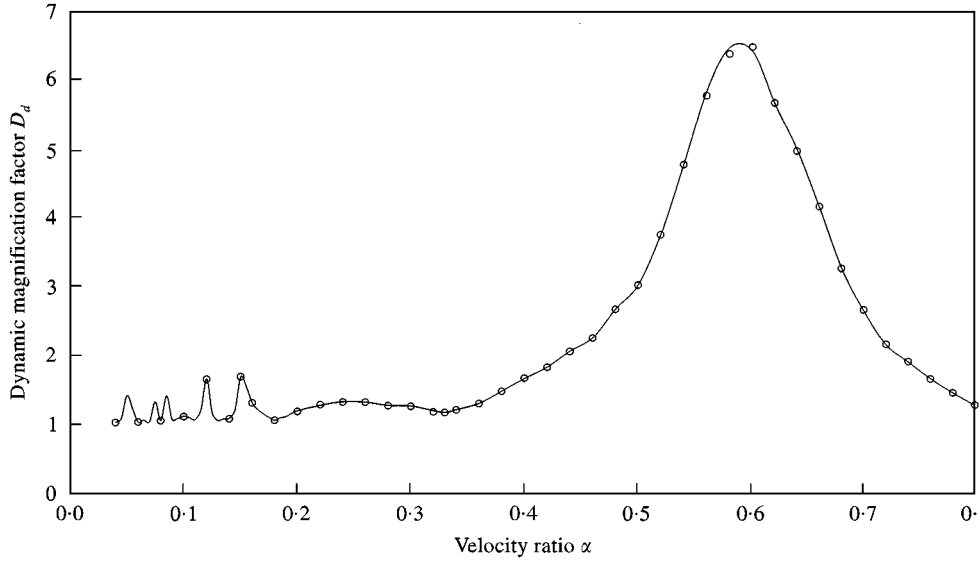


Figure 12. Simply supported bridge under a train modelled as moving forces, dynamic magnification factor $D_d$; ——, present; ○, reference [12].

moving vehicle model predicted effectively the same resonant points and points of cancellation although the dynamic magnification factors do differ a bit.

### 3.4. EXAMPLE 4. A 5-SPAN CONTINUOUS BRIDGE UNDER A MOVING TRAIN

A 5-span continuous prestressed concrete bridge is then considered. Each span is equal to 20 m and all other parameters of the bridge and the train are the same as in Example 3. The train was first modelled as a series of moving forces and solved by the present method using 12 terms and 3200 equal time steps. The problem was

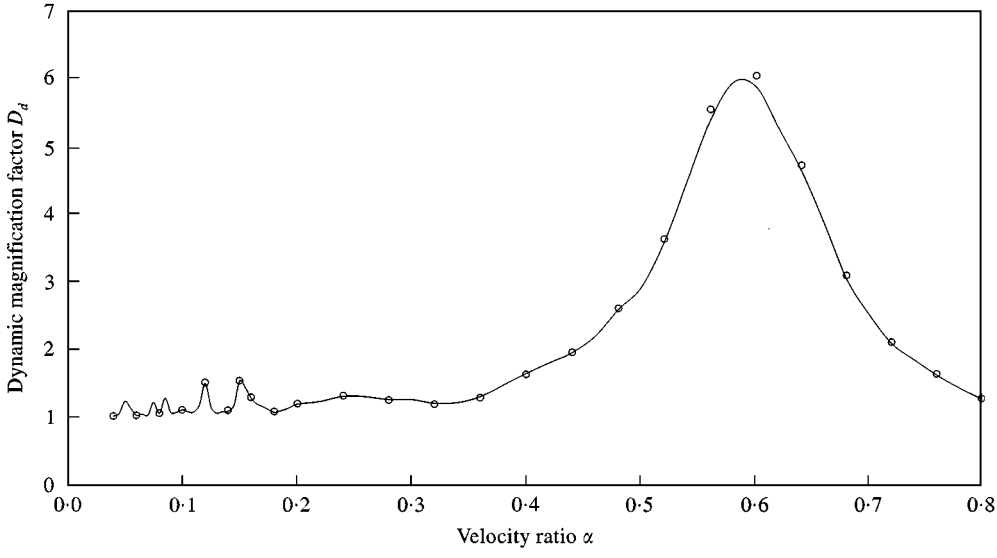


Figure 13. Simply supported bridge under a train modelled as moving vehicles, dynamic magnification factor $D_d$; ——, present; ○, reference [18].

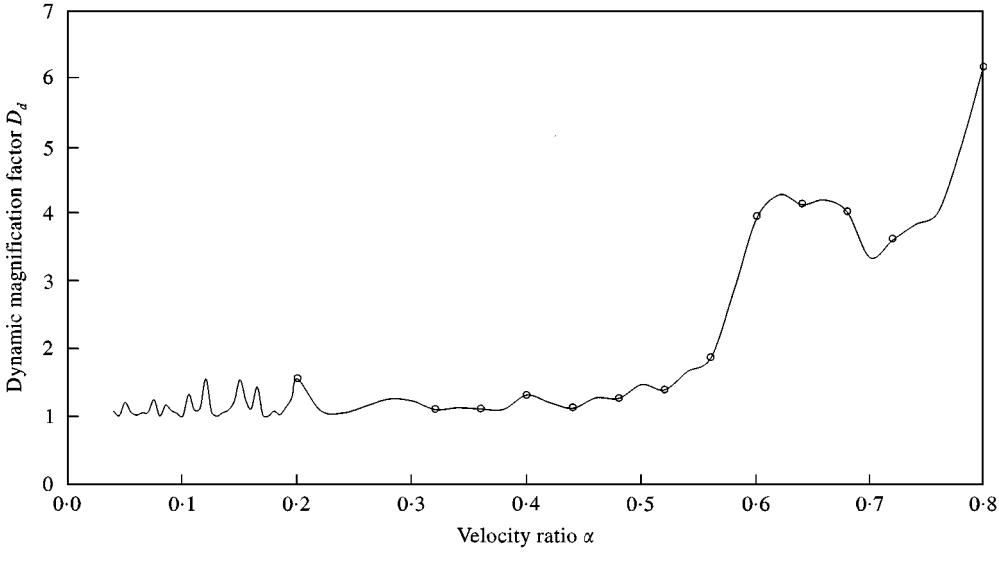


Figure 14. Five-span continuous bridge under a train modelled as moving forces, dynamic magnification factor $D_d$; ——, present; ○, finite element [18].

then re-analyzed using the present method by the moving vehicle model with 16 terms and 3200 equal time steps. Figures 14 and 15 show the dynamic magnification factor for mid-span displacement at the central span $D_d$ obtained by the present method using the moving force model and moving vehicle model, respectively, compared to results obtained from the finite element method [18]

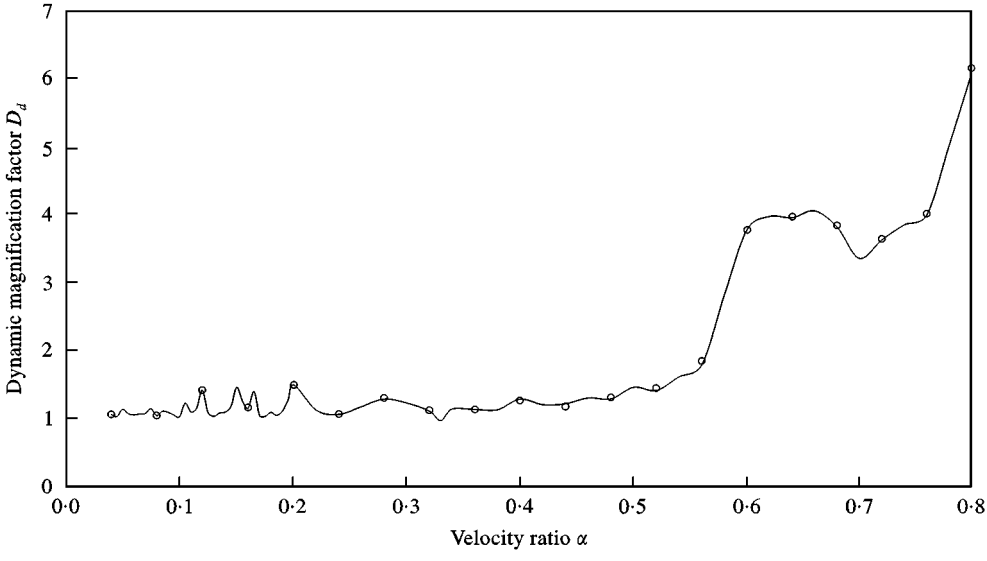


Figure 15. Five-span continuous bridge under a train modelled as moving vehicles, dynamic magnification factor $D_d$; ——, present; ○, finite element [18].

using 80 beam elements of equal lengths. Very good agreement is observed. In addition, it is observed that both the moving force model and the moving vehicle model have predicted effectively the same resonant points and points of cancellation.

## 4. CONCLUSIONS

Based on the Lagrangian approach, the equations of motion of a continuous bridge under moving vehicles and trains have been formulated in matrix form. The modified beam vibration functions are adopted to model the bridge deflection. The modified beam vibration functions satisfy the zero deflection conditions at all the intermediate point supports as well as the boundary conditions at the two ends of the bridge. Compared with the finite element method, the number of unknowns in the present method is much smaller and hence programming is quite straightforward. Numerical results are presented for both prismatic and non-prismatic bridges under a single moving vehicle or convoy, and they agree well with available results. Numerical simulation shows that this method is versatile, accurate and efficient.

## ACKNOWLEDGMENTS

The financial support of the Hong Kong Research Grants Council is acknowledged.

## REFERENCES


1. L. Fryba 1972 *Vibration of Solids and Structures Under Moving Loads*. Groningen, The Netherlands: Noordhoff International Publishing.
2. D. M. Yoshida and W. Weaver 1971 *Publication of International Association for Bridge and Structural Engineering* **31**, 179–195. Finite element analysis of beams and plates with moving loads.
3. F. V. Filho 1978 *Shock and Vibration Digest* **10**, 27–35. Finite element analysis of structures under moving loads.
4. J. Hino, T. Yoshimura, K. Konishi and N. Ananthanarayana 1984 *Journal of Sound and Vibration* **96**, 45–53. A finite element method prediction of the vibration of a bridge subjected to a moving vehicle load.
5. J. Hino, T. Yoshimura and N. Ananthanarayana 1985 *Journal of Sound and Vibration* **100**, 477–491. Vibration analysis of non-linear beams subjected to a moving load using the finite element method.
6. M. Olsson 1985 *Journal of Sound and Vibration* **99**, 1–12. Finite element, modal co-ordinate analysis of structures subjected to moving loads.
7. Y. H. Lin and M. W. Trethewey 1990 *Journal of Sound and Vibration* **136**, 323–342. Finite element analysis of elastic beams subjected to moving dynamic loads.
8. M. Yenerand K. Chompooming 1994 *Computer and Structures* **53**, 709–726. Numerical method of lines for analysis of vehicle–bridge dynamic interaction.
9. K. Chompooming and M. Yener 1995 *Journal of Sound and Vibration* **183**, 567–589. The influence of roadway surface irregularities and vehicle deceleration on bridge dynamics using the method of lines.
10. Y. B. Yang and B. H. Lin 1995 *Journal of Structural Engineering* **121**, 1636–1643. Vehicle–bridge interaction analysis by dynamic condensation method.
11. Y. B. Yang, S. S. Liao and B. H. Lin 1995 *Journal of Structural Engineering* **121**, 1644–1650. Impact formulas for vehicles moving over simple and continuous beams.
12. Y. B. Yang, J. D. Yau and L. C. Hsu 1997 *Engineering Structures* **19**, 936–944. Vibration of simple beams due to trains moving at high speeds.
13. K. J. Bathe and E. L. Wilson 1976 *Numerical Methods in Finite Element Analysis*. NJ, U.S.A.: Prentice-Hall Inc., Englewood Cliffs.
14. G. Sewell 1988 *The Numerical Solution of Ordinary and Partial Differential Equations*. San Diego, CA: Academic Press.
15. M. Paz 1989 *Journal of Structural Engineering* **115**, 234–238. Modified dynamic condensation method.
16. D. Y. Zheng, Y. K. Cheung, F. T. K. Au and Y. S. Cheng 1998 *Journal of Sound and Vibration* **212**, 455–467. Vibration of multi-span non-uniform beams under moving loads by using modified beam vibration functions.
17. Y. K. Cheung and L. G. Tham 1998 *Finite Strip Method*. Boca Raton, FL: CRC Press.
18. Y. K. Cheung, F. T. K. Au, Y. S. Cheng and D. Y. Zheng 1997 *Research Report on Finite Element Analysis of Bridge–Vehicles Interaction*. Department of Civil and Structural Engineering, The University of Hong Kong.


## APPENDIX A: NOTATION

| | |
|---|---|
| $\{c_s, s = 1, 2, \ldots, N\}$ | damping coefficient of the $s$th vehicle |
| $EI(x)$ | flexural rigidity of the bridge |
| $\{f_{cs}(t), s = 1, 2, \ldots, N\}$ | contact force between the $s$th vehicle and the bridge |
| $\{\Delta f_{cs}(t), s = 1, 2, \ldots, N\}$ | fluctuating part of the contact force $f_{cs}(t)$ |
| $\{k_s, s = 1, 2, \ldots, N\}$ | stiffness of the $s$th vehicle |
| $L$ | Lagrangian function of the bridge |
| $\{M_{s1}, M_{s2}, s = 1, 2, \ldots, N\}$ | unsprung mass and sprung mass, respectively, of the $s$th vehicle |

| | |
|---|---|
| $\{m_{ij}, k_{ij}, i, j = 1, 2, \ldots, n\}$ | generalized mass and stiffness matrices of the bridge only |
| $\{m^*_{ij}, c^*_{ij}, k^*_{ij}, i,j = 1, 2, \ldots, n\}$ | generalized mass, damping and stiffness matrices of the bridge with vehicles on it |
| $N$ | number of vehicles in the convoy |
| $\{p^*_i(t), i = 1, 2, \ldots, n\}$ | generalized force |
| $\{q_i(t), i = 1, 2, \ldots, n\}$ | generalized co-ordinates of the bridge |
| $Q$ | $(Q - 1)$ is the total number of intermediate point supports |
| $\{Q^*_i(t), i = 1, 2, \ldots, n\}$ | generalized force acting on the bridge |
| $\{Q^*_{is}(t), i = 1, 2, \ldots, n;$ $s = 1, 2, \ldots, N\}$ | generalized force acting on the bridge by the $s$th vehicle |
| $r(x)$ | surface irreularity function |
| $U$ | bending energy of the bridge |
| $V$ | kinetic energy of the bridge |
| $v(t)$ | velocity of the convoy |
| $w(x, t)$ | deflection of the beam at location $x$ |
| $\{x_s(t), s = 1, 2, \ldots, N\}$ | abscissa of the $s$th vehicle |
| $\{X_i(x), i = 1, 2, \ldots, n\}$ | modified beam vibration functions |
| $\{\bar{X}_i(x), i = 1, 2, \ldots, n\}$ | vibration modes of a hypothetical prismatic beam of length $l$ with the same end support conditions |
| $\{\tilde{X}_i(x, i = 1, 2, \ldots, n\}$ | augmenting cubic spline expressions |
| $\{y_{s1}(t), y_{s2}(t), s = 1, 2, \ldots, N\}$ | vertical displacements of the unsprung mass and sprung mass, respectively, of the $s$th vehicle |
| $\rho A(x)$ | mass per unit length of the bridge |
| $\mathbf{M}_2$, $\mathbf{C}$, $\mathbf{K}$ | vehicle unsprung mass, damping and stiffness matrices |
| $\mathbf{M}^*$, $\mathbf{C}^*$, $\mathbf{K}^*$ | generalized mass, damping and stiffness matrices of the bridge with vehicles on it |
| $\mathbf{p}^*$ | generalized force vector |
| $\mathbf{q}$ | generalized co-ordinate vector for the bridge |
| $\mathbf{r}$ | surface irregularity function vector |
| $\mathbf{X}$ | modified beam vibration function matrix |
| $\mathbf{y}_2$ | vehicle sprung mass displacement vector |